2024 IEEE International Conference on Robotics and Automation (ICRA 2024)
May 13-17, 2024. Yokohama, Japan

High Precision Paint Deposition Modeling Considering Variable Posture of Spray Painting Robot

Genichiro Tanaka, Yoshinobu Takahashi, and Hiroyasu Iwata, *Member, IEEE*

***Abstract*— This study developed a high-precision paint deposition model that considers the position and direction of a spray-painting gun. Our angle-specific paint deposition model focused on the change in paint deposition due to the change in the painting angle; however, there was a problem with its versatility. We analyzed this problem, and the solution was achieved by separately modeling changes in the film thickness distribution using impact angle and spray distance, which were previously modeled together. For higher accuracy, a special function was proposed to convert the three-dimensional vector into two-dimensional coordinate values in the distribution function upper plane. To confirm the validity of our model, a painting test on an L-shaped surface was conducted, and the measured and predicted values were compared. The L-shaped surface is a typical shape in which the film thickness distribution changes with the angle; a complex path with varying distances and angles was employed. The results confirmed that the predicted values agreed well with the measured values in the L-shaped surface painting test, validating the developed model.**

I. Introduction

Painting robots are extensively used in the painting processes of automobiles, ships, aerospace, and surface-strengthening technology, contributing to factory automation [1–3]. However, due to drawbacks such as long working time, uniformity of painting film thickness, painting efficiency, and dependence on operator skill, research on off-line programming of painting robots has become a hotspot [4–6]. In off-line programming technology, the planning of the painting path and optimization of painting parameters are critical, and this task is called teaching. The operator is required to set them according to the required quality. However, there are issues with the lack of standards for teaching planning and the inability to reproduce painting phenomena in a virtual space. To address these issues, research on teaching methods and modeling of painting phenomena is being conducted [7,8]. In addition, modeling of painting phenomena to predict painting film thickness is gaining attention as a first step in robotic painting research. If the paint film thickness can be predicted through simulations, operators can attempt teaching iterations in a virtual space. It can also support research on teaching planning, which is another issue. Zeng et al. used a plane-cutting method to generate thermal spray paths on each approximate plane of the target surface and optimized the spacing distance between adjacent paths and painting speed to improve film thickness uniformity [9]. Klein et al. defined a paint diffusion pattern as a conical model and proposed a teaching method for robotic painting operations [10]. Andulkar et al. developed a painting model called a paint deposition model that can predict the lamination thickness using defined painting paths [14,15]. Additionally, several studies have been conducted to develop teaching methods based on the paint film model to uniformly paint the entire painted surface, individually or otherwise [16–19]. Furthermore, a variable painting gun-angle model has been proposed based on a conventional painting model that assumes the orientation of painting machine to be 90° to the surface to be coated. The abovementioned studies are excellent and have achieved satisfactory results primarily for flat and free-form surfaces, such as automobiles and ships. However, when painting complex shapes, the painting angle and distance to the painted surface change as the painting gun moves, which cannot be handled by conventional models. A complex target could be a construction machine composed of multiple planes or L-shaped surfaces. To paint a complex geometry, a painting model, which reflects the effect of changes in the relative position and orientation of the painting gun and the surface to be coated on the painting, is required. Therefore, we proposed an angle-specific paint deposition model based on our previous study on paint deposition models [20]. This model is referred to as “our previous model” in this study. This model enables film thickness predictions for L-shaped surface painting and considers the posture of the painting gun. However, it is applicable only within a certain range, which is problematic from versatility viewpoint. To solve this problem, a different method was adopted, and a highly versatile paint deposition model was required.

Fig. 1. This picture shows the painting robot used in this study. The painting robot has a painting gun attached at the end of its robot arm.

*Research supported by ABC Foundation.

Genichiro Tanaka is Graduate School of Creative Science and Engineering, Waseda University, 27 Waseda-cho, Shinjuku-ku, Tokyo 162-0042, Japan (corresponding author; Phone: +81-3-3203-4427; Fax: +81-3-3203-4427; E-mail: genichiro2077@asagi.waseda.jp).

Yoshinobu Takahashi is Graduate School of Creative Science and Engineering, Waseda University, 27 Waseda-cho, Shinjuku-ku, Tokyo 162-0042, Japan (corresponding author; Phone: +81-3-3203-4427; Fax: +81-3-3203-4427; E-mail: takayoshi-jean@akane.waseda.jp).

H. Iwata is with the Faculty of Science and Engineering, Waseda University, 27 Waseda-cho, Shinjuku-ku, Tokyo 162-0042, Japan (E-mail: jubi@waseda.jp).

The objective of this study is to develop a highly accurate paint deposition model for predicting the thickness of a painting film when multiple surfaces are painted continuously. In this study, we develop a general-purpose paint deposition model that can be used to specify the orientation and distance of the painting gun. Although we have previously studied paint film flow [21], in this study, we assume that paint adheres to the surface and no flow occurs. The painting machine used in this study was an automatic painting gun [22] with a robotic arm [23] and an airless spray system (Fig. 1). The validity of the proposed model is verified by complex painting paths using a typical complex shape, L-shaped surface, as the painting target.

II. Research Methods

In this chapter, the problems of the proposed old angular paint deposition model are clarified and a new method for improving the problem is presented. The limitations of the previous model were described in previous studies, and the limitations are analyzed numerically to clarify the specific causes. Then, based on the results of the analysis, elaborative solutions are presented.

A. Analysis of Issues with Previous Angle-Specific Paint Deposition Model

In our previous model, an angle-specific paint deposition model was developed by multiplying the film thickness distribution function, which applies the bivariate Gaussian distribution [24] proposed by Freund et al. The angle correction formula f is as follows.

$$f(x,y) = p_0 + p_1 x + p_2 y + p_3 x^2 + p_4 xy + p_5 y^2 \quad (1)$$

$$x = \frac{\theta_c}{90}, y = \frac{d_{wg}}{300}, f(x,y) = \frac{q}{q_{pre}}$$

The modified formula f is multiplied by the film thickness at a gun angle of 90° to calculate the film thickness for each angle. (1) includes the impact angle (θ_c) and spray distance (d_{wg}) and expresses how much the lamination thickness (q_{pre}) on the distribution function plane varies with the actual lamination thickness (measured value) q on the surface of the target. Traditionally, the film thickness for each angle is calculated by multiplying the film thickness at a gun angle of 90° by modified formula f. Analysis of painting phenomena has revealed that the impact angle (θ_c) and spray distance (d_{wg}) have a significant influence on the film thickness distribution depending on the position and posture of the painting gun. Therefore, we derived a modified equation f by performing multiple regression analyses with θ_c and d_{wg} as explanatory variables and q/q_{pre} as the objective variable. Validation showed that the average error rate was 8.58%, indicating validity. However, because a polynomial equation is used for the modified formula f, there is a possibility that issues may arise when more complex painting is performed. In addition, since it is obtained by regression from limited input data, it is a biased fitting and is considered to have generalizability problems.

Therefore, the range of inapplicability is clarified by graphing the values obtained using the modified formula f. We mapped the values obtained using the modified formula f of our previous model in the ranges of spray distance (200–800 mm) and impact angle (30°–90°) (Fig. 2).

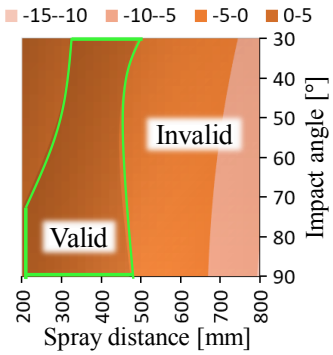

Fig. 2. The graph showing the values obtained by the modified formula f in Our previous model. The range of spray distance (200~800mm) and impact angle (30~90°) are shown.

Fig. 2 shows that the value obtained using the modified formula f is positive within the range enclosed by the line, whereas f obtains a negative value outside the range. In other words, our previous model does not obtain valid values when the spray distance exceeds approximately 500 mm.

The actual painting is considered to be performed in three-dimensional (3D) coordinates; however, the basic film thickness distribution function is two-dimensional (2D). Therefore, the painting path and targets are limited, and the model can be applied under limited conditions, making it a model with low generalizability. Therefore, it is necessary to consider a paint deposition model with a broad effective range and high generalizability. The policy for a new paint deposition model is described in the next section.

B. New Methodology for Deriving Advanced Angle-Specific Paint Deposition Model

Similar to our previous model, this study models the paint spray shape as an elliptic cone using a film thickness distribution function and calculates the film thickness at each point. A two-variable Gaussian function is used as the film thickness distribution function, with an additional twist in the constant term.

$$q(x,y) = \frac{Q}{2\pi\sigma_x\sigma_y}\exp\left\{-\frac{1}{2}\left[\left(\frac{x-x_0'}{\sigma_x}\right)^2 + \left(\frac{y-y_0'}{\sigma_y}\right)^2\right]\right\} \quad (2)$$

Here, Q represents the discharge flow rate of paint [m^3/s], σ_x and σ_y denotes coefficients, x and y represents the coordinates of each point on the target, and x_0' and y_0' denote the coordinates of Gaussian distribution center. The coefficients of the exp term are designed to ensure that the volume of the region bounded by Gaussian surface and $x-y$ plane remain constant as σ_x and σ_y are varied. In other words, if the discharge flow rate is constant, the output of a film thickness distribution corresponding to changes in the gun distance is possible simply by changing σ_x and σ_y. In other words, the following equation, whose proof is omitted, is valid. A schematic of this phenomenon is shown in Fig. 3.

$$\int_{-\infty}^{\infty}\int_{-\infty}^{\infty} q(x,y)\,dx\,dy = Q \quad (3)$$

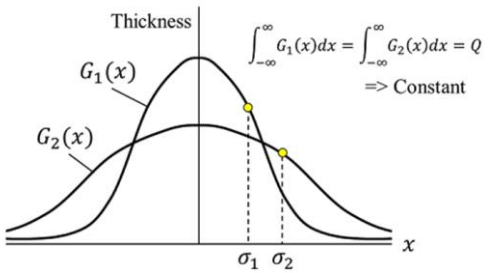

Fig. 3. Schematic representing the constraints of film thickness distribution function (2D display)

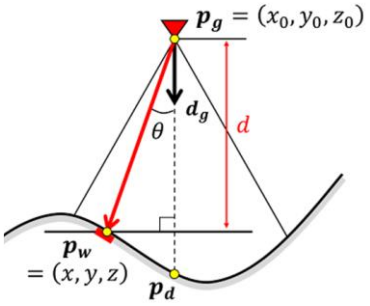

Fig. 4. Geometric schematic representing an example of a painting scene; red triangle represents the painting gun.

As an example, consider the situation shown in Fig. 4, where $\boldsymbol{p_g}$ denotes the position vector of the painting gun tip, $\boldsymbol{p_d}$ denotes the position vector of the intersection of the painting gun projectile and the target, and $\boldsymbol{p_w}$ denotes the position vector of each point on the target. The equation for calculating the film thickness at the position $\boldsymbol{p_w}$ is considered. In the Gaussian distribution function (2), (x_0', y_0') corresponds to $\boldsymbol{p_d}$ and (x, y) corresponds to $\boldsymbol{p_w}$.

Based on the above basic theory and the analysis results of our previous model, we present two major improvements and derive an advanced paint deposition model. The position coordinates of the target input in (2) are two-dimensional coordinate values in the plane on the distribution function, but the actual painting phenomenon is a three-dimensional vector in the absolute coordinate system. Although this point has not been improved from our previous model, we propose a function that converts 3D vectors into 2D coordinate values in the distribution function plane to construct a more advanced paint deposition model.

Second, in the past, changes in the film thickness distribution with the impact angle and jetting distance were modeled together using multiple regression analysis. However, because these changes are related to different factors, overfitting occurred in our previous model. Therefore, by modeling the two phenomena separately, a highly precise paint deposition model is developed.

III. Theory and Modeling

This chapter discusses three theories to achieve the two improvements described in the previous section: a theory that transforms a 3D vector into 2D coordinates on the distribution function, and a theory that models changes in the film thickness distribution with the impact angle and spray distance.

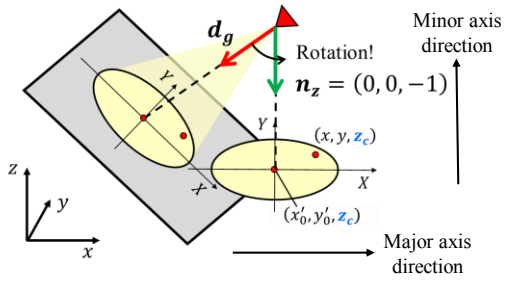

Fig. 5. Schematic showing two-dimensionalization of distribution function due to coordinate system rotation; it also shows moving direction with respect to elliptical shape of paint distribution.

A. Coordinate System Transformation Method

While $\boldsymbol{p_d}$ and $\boldsymbol{p_w}$ input to (2) are 3D vectors in the absolute coordinate system, the coordinate values input to Gaussian distribution function are 2D coordinate values in the plane above the distribution function. Therefore, it is necessary to prepare a transformation function to convert the former values to the latter. Here, the policy is to align the z-coordinate values of $\boldsymbol{p_d}$ and $\boldsymbol{p_w}$. As depicted in Fig. 5, by rotating the direction vector $\boldsymbol{d_g}$ of the painting gun to match the unit vector $\boldsymbol{n_z}$ parallel to z-axis, $\boldsymbol{p_d}$ and $\boldsymbol{p_w}$ should automatically be on $x - y$ plane. In other words, we can find a rotation matrix R such that $\boldsymbol{d_g}$ can be superimposed on $\boldsymbol{n_z}$. Therefore, Rodriguez rotation formula is used to calculate the rotation matrix R. According to the above formula, a point $\boldsymbol{r}'$ in 3D space with $\boldsymbol{n}$ as the axis and $\boldsymbol{r}$ rotated by θ can be expressed as follows:

$$\boldsymbol{r}' = (\cos\theta)\boldsymbol{r} + (1 - \cos\theta)(\boldsymbol{r} \cdot \boldsymbol{n})\boldsymbol{n} + (\sin\theta)(\boldsymbol{n} \times \boldsymbol{r}) \quad (4)$$

Expressed in terms of rotation matrix R_θ, R_θ is a map that transforms the vector $\boldsymbol{r}$ into $\boldsymbol{r}'$, where $\boldsymbol{n} = (n_x, n_y, n_z)$, as follows:

$$R_\theta = (1 - \cos\theta)\begin{bmatrix} {n_x}^2 & n_x n_y & n_x n_z \\ n_x n_y & {n_y}^2 & n_y n_z \\ n_x n_z & n_y n_z & {n_z}^2 \end{bmatrix} + \begin{bmatrix} \cos\theta & -n_z \sin\theta & n_y \sin\theta \\ n_z \sin\theta & \cos\theta & -n_x \sin\theta \\ -n_y \sin\theta & n_x \sin\theta & \cos\theta \end{bmatrix} \quad (5)$$

For (5), consider the case where the two vectors $\boldsymbol{r}$ and $\boldsymbol{r}'$ are given from the beginning and are, in particular, unit vectors. If the axis of rotation $\boldsymbol{n}$ lies in the plane in which the above two vectors exist, $\boldsymbol{n}$ lies exactly in the middle of the two vectors (on the bisector of the angle formed by the two vectors), and the following equation is obtained:

$$\boldsymbol{n} = \frac{\boldsymbol{r} + \boldsymbol{r}'}{\|\boldsymbol{r} + \boldsymbol{r}'\|} \quad (6)$$

In this case, $\boldsymbol{r}'$ denotes the vector obtained when $\boldsymbol{r}$ is rotated 180° around this axis, and Rodriguez rotation formula is valid. Based on the above, the following equation is obtained by applying (5) with I as the unit matrix:

$$R_\theta = 2\left[\frac{(\boldsymbol{r} + \boldsymbol{r}') \otimes (\boldsymbol{r} + \boldsymbol{r}')}{\|\boldsymbol{r} + \boldsymbol{r}'\|^2}\right] - I \quad (7)$$

In conclusion, because the rotation matrix can be obtained by applying $\boldsymbol{d_g}$ and $\boldsymbol{n_z}$ to $\boldsymbol{r}$ and $\boldsymbol{r}'$ in (7), this rotation matrix R_θ

can be multiplied by $\boldsymbol{p_d}$ and $\boldsymbol{p_w}$. The film thickness distribution function can be calculated at any point on the target.

B. Film Thickness Calculation Considering Gun Distance

The shape of the paint deposition model varies with the constant Q and values of σ_x and σ_y. When only gun distance changes, the discharge flow rate does not change; thus, σ_x and σ_y values can be made dependent on the gun distance values. As depicted in Fig. 6, σ_x and σ_y values are large when the gun distance is large, indicating a positive correlation between the two. A theory is developed for this relationship. In this theory, the paint spray shape is modeled as an elliptic cone; thus, the spray should look as shown in Fig. 6 when viewed from the side. Since a Gaussian distribution is used for film thickness distribution, σ_x and σ_y correspond to the "standard deviation" in general statistics. Using the concept of "confidence interval" here, we can obtain the following relationship equation when the mean value is μ.

$$\mu - 3\sigma \leq x \leq \mu + 3\sigma \tag{8}$$

The data within this range represent approximately 99.7% of the population. On this basis, the range where most particles adhere is $\pm 3\sigma$ from the center, as depicted in Fig. 6, when the data are replaced with paint particles. In other words, theoretically, the gun distance d and constants σ_x and σ_y are in a proportional relationship. However, the above is only a theory, and in practice, it is not always a perfect linear relationship. Therefore, we considered modeling based on actual measurements of the film thickness when the gun distance varied. The following equations model σ_x and σ_y:

$$\sigma_{x,y}(d) = \left(\frac{d}{\bar{d}}\right)^{\alpha} \bar{\sigma}_{x,y} \tag{9}$$

where $\bar{d}$ and $\bar{\sigma}_{x,y}$ denote the reference gun distance and constant. The value of $\bar{\sigma}_{x,y}$ is identified based on the measured film thickness distribution when painting at a certain gun distance $\bar{d}$. Since this value depends on the painting gun and nozzle used, parameter identification must be performed. In addition, the linearity α between the gun distance d and constants σ_x and σ_y is identified from measured film thickness distribution when the painting gun distance varies in several ways. The value of α is theoretically independent of the painting gun, and the theoretical value of α is 1.

C. Film Thickness Calculation Considering Gun Angle

Here, we model the effect of the change in the film thickness distribution due to the impact angle θ_c. In the model of a previous study [25], the modified equation is approximated using a second-order polynomial; however, as overfitting may occur during parameter identification, resulting in a model that does not fit the theory, the present model employs the following simple power-of-fact approximation:

$$q'(x, y, \theta_c) = q(x, y)\left(\frac{\theta_c}{90}\right)^{p} \tag{10}$$

Note that θ_c denotes the impact angle [deg] and p represents a positive constant. The value of p can be identified experimentally. To calculate the impact angle θ_c at each point on the target, consider the normal vector $\boldsymbol{n_w}$ at a point on the target, as depicted in Fig. 7, and define the impact angle as the angle between the plane perpendicular to this normal vector (tangent plane) and the vector connecting the gun tip to a point on the target. In this case, θ_c is the value of the angle between the two vectors minus 90°.

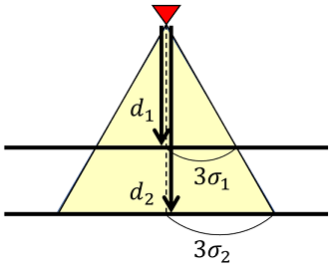

Fig. 6. Geometric schematic representing relationship between gun distance d and constant σ

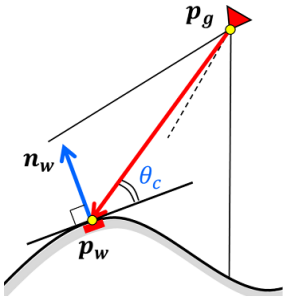

Fig. 7. Schematic showing definition of impact angle and geometric model of painted scene

$$\theta_c = \frac{180}{\pi}\cos^{-1}\frac{\boldsymbol{n_w}\cdot(\boldsymbol{p_w}-\boldsymbol{p_g})}{\|\boldsymbol{n_w}\|\,\|\boldsymbol{p_w}-\boldsymbol{p_g}\|} - 90 \tag{11}$$

However, if the angle between the two vectors is less than 90° (for example, if the paint is to be applied to the back side of the target), the value of θ_c becomes negative. In this case, the paint will not adhere; thus, a conditional branch can be set so that the value of the film thickness is set to 0. For p, the same parameter identification test as that conducted for our previous model was conducted. The result was $p = 0.701$, which is the value used in this study.

IV. Validation of The Simulation

From the theory in Chapter 3, the value of film thickness H_{ij} at any calculated point on the target, generated by the painting gun at an arbitrary time t, can be calculated from the following equation, where Δt denotes the time step of gun position change.

$$H_{ij} = \frac{Q}{2\pi\sigma_x\sigma_y}\exp\left\{-\frac{1}{2}\left[\left(\frac{x-x_{0'}}{\sigma_x}\right)^2 + \left(\frac{y-y_{0'}}{\sigma_y}\right)^2\right]\right\}\left(\frac{\theta_c}{90}\right)^{p}\Delta t \tag{11}$$

Note that each parameter can be calculated from the target and painting gun information; however, $\sigma_{x,y}$ is calculated based on (9). A simulation is performed based on (11), and the film thickness distribution on the target can be predicted numerically and with a heat map.

In this chapter, the validity of the developed high-precision

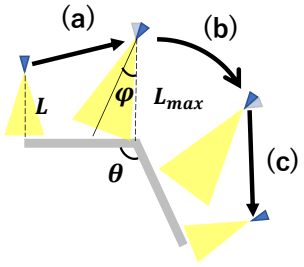

Fig. 8. Schematic showing the target, paint path, in the validation; it includes important parameters in paint path

TABLE I. CONDITIONS FOR MEASUREMENT TESTS IN VALIDATION

	Item	Value
Experimental painting conditions	***Paint***	Urethane resin paint
	Paint viscosity	0.18 Pa s
	Discharge pressure	0.15 MPa
	Pattern air pressure	0.225 MPa
	Wrapping air pressure	0.08 MPa
	Target plate	2 Steel flat plates $300 \times 300 \times 0.6$ mm^2
	Target intersection angle θ	90, 135°
	Moving direction	Minor axis direction
	Gun-to-target distance L	350 mm
	Maximum Gun-to-target distance L_{max}	500 mm
	Corner gun angle φ	15, 10°
	Gun speed	444, 300 mm/s

paint deposition model is verified by comparing simulation results with the actual film thickness distribution when changes in film thickness distribution occur due to the changes in painting gun posture. First, the setup and test conditions of the actual measurement test using the painting gun are discussed, and the results of the film thickness measurements are presented. Next, the setup and conditions for numerical calculations are presented, and the analytical results are discussed. Finally, these results are compared and discussed.

A. Experimental Setup

Tests are conducted on targets and painting routes with significant changes in the film thickness distribution due to the painting gun posture. The validation setup includes a continuous painting path shown in Fig. 8 for two types of L-shaped surfaces with crossing angles of 90° and 135°. The L-shaped surface is significantly affected by changes in the painting gun posture. First, the painting gun is moved from the edge of the upper half of L-shaped surface to the corner in a one-path form, varying the gun distance L_{max} and painting angle φ (a). Next, the painting gun is rotated with the gun distance fixed concerning the corner (circular motion with the corner as the center of the circle) and moved at an equal angular velocity until it reaches the lower half of L-shaped surface and φ (b). Finally, a one-path motion of the painting gun is performed on the lower half of L-shaped surface (c) in

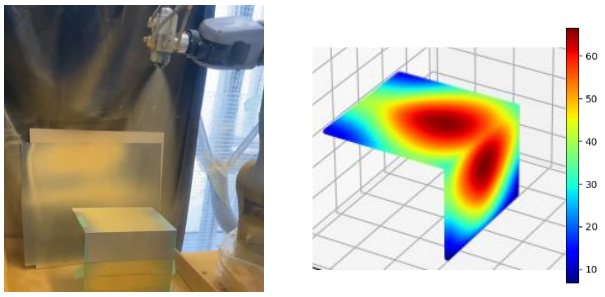

(a) (b)

Fig. 9. Pictures showing (a) measurement tests in validation and an example of a heat map (b) obtained from simulation; figure shows situation at target intersection angle of 90°

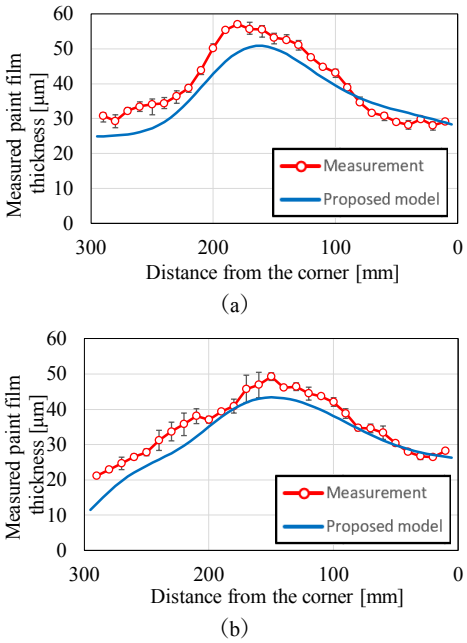

Fig. 10. Paint film thickness measurement results of L-shaped painting experiments and film thickness prediction results of simulation; graph shows film thickness distribution in center of target; (a) shows results for a target intersection angle of 90°, and (b) shows the results for a target intersection angle of 135°.

the same manner as in (a). The painting conditions in the test are presented in Table I. In Fig. 9, two experiments were conducted by varying θ and φ with L and L_{max} as fixed conditions. In the experiment, $\varphi = 15°$ when $\theta = 90°$ and $\varphi = 10°$ when $\theta = 135°$. Tests were conducted twice each under the same conditions to account for variations in the results. After the painted surface dried, 29 points were measured at 10-mm intervals along the center portion of the pattern width from the corners of the top surface. Furthermore, to account for mechanical errors in the displayed value of the film thickness gauge, two measurements were taken at each measurement point, and the average value of these measurements was used. An example of the actual equipment test and heat map output from the simulation is depicted in Fig. 9.

B. Experimental Results

The painting and analysis results of the film thickness distribution obtained from the actual test and simulation are presented in Fig. 10. The measured values are plotted on the graph as the average of all trials, and the minimum and maximum values of measured values in the trials are shown as error bars. The measured values are compared with the predicted values obtained from the simulation of the proposed model. The average error rate between the measured values and proposed model was 12.2% for $\theta = 90°$ and 12.5% for $\theta = 135°$. Simulations were also performed using our previous model. However, as shown in Fig. 2, normal values could not be obtained at a impact distance of 500 mm, making prediction impossible.

C. Discussion

Validation considerations include an evaluation of the accuracy of predictions. The average error rate were 12.2% and 12.5% for the proposed model, which employed the high-precision paint deposition model, and high accuracy was obtained in all cases. Even under conditions where it was impossible to predict with our previous model, the proposed model could make predictions with high accuracy, confirming its validity. Theoretically, the model can handle arbitrary distances and angles, and its validity was confirmed even for paths with continuously varying distances and angles, making it a highly versatile model. The validation test evaluated the model on an L-shaped surface. The results suggest that the model can make predictions with high accuracy even for more complex shapes consisting of multiple surfaces.

Finally, we discuss the limitations of this study. We assumed that the target consisted of surfaces with no unevenness. However, when there are protrusions such as cylinders, it is necessary to consider the shadowed areas. In the proposed model, shadows are not considered. Therefore, if a painting is applied at an angle to a protruding cylindrical shape, the painting thickness will be applied to the shadow areas where the painting would not normally be applied. To solve this problem, it is necessary to mathematically derive and model these shadow areas. We believe that solving this problem will possibly predict the film thickness for any target and under any condition. Furthermore, because the film thickness can be predicted for arbitrary targets and routes, it can be used to derive the optimal painting route to paint a target. Therefore, it is necessary to conduct validation tests under additional test conditions in the future, and route planning using film thickness prediction will be of great value as the next step.

V. Conclusion

This study focused on the versatility of painting gun attitude and distance, which was a major issue in our previous model. The effects of the impact distance and angle, which change the film thickness distribution, were modeled together; however, by modeling them separately, a more advanced film thickness prediction model could be constructed. First, we analyzed the challenges of our previous model and presented a methodology to overcome them. Then, three theories to address the issues were presented with figures and equations. Finally, to evaluate the validity of the high-precision paint deposition model, we compared the actual film thickness distribution when an L-shaped surface was painted with the prediction results obtained using angle-specific paint deposition model. The results showed that film thickness prediction was possible for painting of L-shaped surfaces, where the film thickness distribution changes depending on the position and posture of the painting gun. Furthermore, the system can handle a wide range of impact angles and distances, confirming its high versatility.

The goal of this research was to predict film thickness for any given position and orientation of a painting gun on any complex geometry, using highly accurate simulations to assist in setting routes and painting conditions. We believe that we have largely achieved our goal in this study. The proposed model provides significant potential for routing strategies considered in previous studies. To fully achieve our goal, it is necessary to model the influence of the shadowed part of the projection shape. Combined with our work on painting flow, this will add depth to future studies. Achieving these goals will make robotic painting operations more efficient and assist workers in industrial settings.

Acknowledgment

The authors would like to thank the Research Institute of Science and Engineering, Waseda University, for providing the space for the experiments.

References

[1] L. Ning and G. L. Wang, “Research on automatic spraying process of aviation products,” Aeronaut. Manuf. Technol., vol. 61, no. 12, pp. 59–64, Jun. 2018.

[2] Z. Cai, H. Liang, S. Quan, S. Deng, C. Zeng, and F. Zhang, “Computer-aided robot trajectory auto-generation strategy in thermal spraying,” J. Thermal Spray Technol., vol. 24, no. 7, pp. 1235–1245, Oct. 2015.

[3] D. D. Fang, Y. Zheng, B. Zhang, X. Li, P. Ju, H. Li, and C. Zeng, “Automatic robot trajectory for thermal-sprayed complex Surfaces,” Adv. Mater. Sci. Eng., vol. 2018, Jul. 2018, Art. no. 86975056.

[4] H. Chen and N. Xi, “Automated robot tool trajectory connection for spray forming process,” J. Manuf. Sci. Eng., vol. 134, no. 2, pp. 021017-1–021017-9, Apr. 2012.

[5] B. Zhou, L. Qian, Z. D. Meng, and X. Z. Dai, "Path sorting optimization of painting robot based on ant colony algorithm," Comput. Eng., vol. 38, no. 1, pp. 192–207, Jan. 2012.

[6] P. Zhang, J. Gong, N. Huifeng, Y. Li, L. Wei, Y. Zeng, and Y. Liu, “Study on trajectory combination and connection problems of spray-painting robot for large curvature combination surfaces,” J. Sichuan Univ., Eng. Sci. Ed., vol. 48, no. 4, pp. 217–222, Jul. 2016.

[7] Z. Bo, Z. Xi, M. Zhengda, D. Xianzhong, “Off-line Programming System of Industrial Robot for Spraying Manufacturing Optimization,” Chinese Control Conference, 2014.

[8] Y. Chen, W. Chen, B. Li, G. Zhang, W. Zhang, “Paint thickness simulation for painting robot trajectory planning,” Industrial Robot, vol. 44, no. 5, pp. 629-638, 2017.

[9] Y. Zeng, Y. Yu, X. Zhao, Y. Liu, J. Liu1, A. D. Liu, “Trajectory planning of spray gun with variable posture for irregular plane based on boundary constraint,” IEEE Access, vol. 9, pp. 52902-52912, 2021.

[10] A. Klein, “CAD-Based off-line programming of painting robots,” *Robotica*, 1987, pp. 267-271.

[11] P. N. Atkar, A. Greenfield, D. C. Conner, H. Choset, A. A. Rizzi, “Uniform coverage of automotive surface patches,” The International Journal of Robotics Research, vol. 24, no. 11, pp. 883-898, 2005.

[12] P. N. Atkar, A. Greenfield, D. C. Conner, H. Choset, A. A. Rizzi, “Uniform coverage of simple surfaces embedded in for auto-body painting” Algorithmic Foundations of Robotics, pp. 27-42, 2005.

[13] D.C. Conner, P.N. Atkar, A.A. Rizzi, H. Choset, “Development of deposition models for paint application on surfaces embedded in IR3 for use in automated path planning,” International Conference on Intelligent Robots and Systems, vol. 2, 2002.

[14] M. V. Andulkar, S. S. Chiddarwar, “Novel integrated offline trajectory generation approach for robot-assisted spray painting operation,” Journal of Manufacturing Systems, vol 37, pp. 201-216, 2015.

[15] M. V. Andulkar, S. S. Chiddarwar, A. S. Marathe, “Incremental approach for trajectory generation of spray painting robot,” Industrial Robot: An n International Journal vol.42, no.3, pp. 228-241, 2015.

[16] H. Chen, N. Xi, Z. Wei, Y. Chen, J. Dahl, “Robot trajectory integration for painting automotive parts with multiple patches,” lEEE International Conference on Robotics & Automation, vol. 3, pp. 3984-3989, 2003.

[17] W. Xia, C. Wei, X. Liao, “Surface segmentation based intelligent trajectory planning and control modeling for spray painting,” IEEE International Conference on Mechatronics and Automation, pp. 4958-4963, 2009.

[18] W. Chen, X. Wang, H. Liu, Y. Tang, J. Liu “Optimized Combination of Spray Painting Trajectory on 3D Entities,” Electronics, vol. 8, no. 1, 74, 2019.

[19] X. Yu, Z. Cheng, Y. Zhang, L. Ou “Point cloud modeling and slicing algorithm for trajectory planning of spray painting robot,” Robotica, vol. 39, no. 12, pp. 2246-2267, 2021.

[20] G. Tanaka, F. Chang, Y. Takahashi, F, Kato, H. Iwata, " Angle-specific paint deposition modeling for an L-shaped plane with the variable posture of a painting gun", *IEEE 11th International Conference on Control, Mechatronics and Automation* (accepted), 2023.

[21] Y. Takahashi, Fangshou Chang, Fumihiro Kato, Hiroyasu Iwata, "Analysis of Paint Film Thickness Distribution Based on Particle Method Considering Time Series Change of Flow", *Proc. of IEEE 18th International Conference on Automation Science and Engineering*, pp. 397-404, 2022.

[22] Asahi Sunac Corporation, “AGA10” [Online]. Available: https://www.sunac.co.jp/en/products/aga10/ [Accessed: March 5 2024]

[23] DENSO, DENSO WAVE, “VS068/087”[Online]. Available: https://www.densorobotics-europe.com/product-overview/products/5-and-6-axis-robots/vs-068-087 [Accessed: March 5 2024]

[24] E. Freund, D. Rokossa, J. Roßmann, “Process-oriented approach to an efficientoff-line programming of industrial robots.,” Proceedings of the 24th annual conference of the IEEE industrial electronics society, vol. 1, pp. 208-213, 1998.

[25] J. Antonio, “Optimal trajectory planning for spray painting,” Proceedings of the 1994 IEEE International Conference on Robotics and Automation, pp. 2570–2577, 1994.